Second-Order Cone Programming for Optimal Power Flow in VSC-Type AC-DC Grids

Mohamadreza Baradar, *Student Member, IEEE*, Mohammad Reza Hesamzadeh, *Member, IEEE*, and Mehrdad Ghandhari, *Member, IEEE*

***Abstract*—This paper presents a second order cone programming (SOCP) formulation of the optimal power flow problem for AC-DC systems with voltage source converter (VSC) technology. Approximation techniques have been used to derive the SOCP formulation of the AC-DC OPF problem. Later, the SOCP formulation can be solved using the interior point method (IPM) by considering the limits on AC-DC grid. The accuracy of SOCP formulation of AC OPF has been proven with numerical examples using IEEE 14-bus, IEEE 30-bus, and IEEE 57-bus example systems. The results of the SOCP formulation are compared with available commercial software. Then a DC system with VSC technology is modeled in the IEEE 30-bus example system. The SOCP formulation of AC-DC OPF is applied to the modified IEEE 30-bus example system and the results are discussed. The limitations of derived SOCP formulation are also discussed.**

***Index Terms*—AC-DC optimal power flow, multi-terminal HVDC systems, second-order cone programming.**

NOMENCLATURE

$n_{b_{AC}}$	Number of AC buses.
$n_{b_{DC}}$	Number of DC buses and converters.
n_G	Number of generators.
$n_{l_{AC}}$	Number of AC lines.
$n_{l_{DC}}$	Number of DC lines.
θ_{sr_j}	Difference phase angle between sending and receiving ends at AC line jth.
κ	Set of convex cones.
$\boldsymbol{C}$	Loop matrix.
n_c	Number of independent loops in AC network.
$\boldsymbol{A}$	Vector of coefficients.
$\boldsymbol{M_{PQ}}$	Incidence matrix associated with AC line active powers with size of $n_{b_{AC}} \times n_{l_{AC}}$.
$\boldsymbol{M_l}$	Incidence matrix associated with AC line active power losses with size of $n_{b_{AC}} \times n_{l_{AC}}$.
$\boldsymbol{P_G}$	Vector of active power generation at each AC bus with size of $n_{b_{AC}} \times 1$ which has only n_G non-zero elements.
$\boldsymbol{Q_G}$	Vector of reactive power generation at each AC bus with size of $n_{b_{AC}} \times 1$ which has only n_G non-zero elements.
$\boldsymbol{P_D}$	Vector containing active power loads at each AC bus with size of $n_{b_{AC}} \times 1$.
$\boldsymbol{Q_D}$	Vector containing reactive power loads at each AC bus with size of $n_{b_{AC}} \times 1$.
$\boldsymbol{P_{r,AC}}$	Vector containing AC line flow active powers at receiving end of AC lines (P_{r,AC_j}) with size of $n_{l_{AC}} \times 1$.
$\boldsymbol{Q_r}$	Vector containing AC line flow reactive powers at receiving end of AC lines (Q_{r_j}) with size of $n_{l_{AC}} \times 1$.
$\boldsymbol{P_{loss,AC}}$	Vector containing AC line flow active power losses (P_{loss,AC_j}) at AC lines with size of $n_{l_{AC}} \times 1$.
$\boldsymbol{Q_{loss,AC}}$	Vector containing AC line flow reactive power losses at AC lines (Q_{loss,AC_j}) with size of $n_{l_{AC}} \times 1$.
$\boldsymbol{M_{P,DC}}$	Incidence matrix associated with DC line active powers with size of $n_{b_{DC}} \times n_{l_{DC}}$.
$\boldsymbol{M_{l_{DC}}}$	Incidence matrix associated with DC line active power losses with size of $n_{b_{DC}} \times n_{l_{DC}}$.
$\boldsymbol{P_{r,DC}}$	Vector containing DC line flow active powers at receiving end of DC lines (P_{r,DC_j}) with size of $n_{l_{DC}} \times 1$.
$\boldsymbol{P_{loss,DC}}$	Vector containing DC line flow active power losses at DC lines (P_{loss,DC_j}) with size of $n_{l_{DC}} \times 1$.
$\boldsymbol{B}$	Diagonal matrix whose elements $B_{i,i}$ are shunt susceptance AC nodes with size of $n_{b_{AC}} \times n_{b_{AC}}$.
$\boldsymbol{R}$	Diagonal matrix whose elements $R_{j,j}$ are resistance of AC lines with size of $n_{l_{AC}} \times n_{l_{AC}}$.
$\boldsymbol{R_{DC}}$	Diagonal matrix whose elements $R_{DC_{j,j}}$ are resistance of DC lines with size of $n_{l_{DC}} \times n_{l_{DC}}$.
$\boldsymbol{X}$	Diagonal matrix whose elements $X_{j,j}$ are reactance of AC lines with size of $n_{l_{AC}} \times n_{l_{AC}}$.
$\boldsymbol{P_{CONV}}$	Injected/absorbed active power vector of converters at PCCs.

Manuscript received November 01, 2012; revised March 04, 2013 and May 13, 2013; accepted June 22, 2013. Date of publication July 30, 2013; date of current version October 17, 2013. Paper no. TPWRS-01226-2012.

The authors are with KTH Royal Institute of Technology, School of Electrical Engineering, Department of Electric Power Systems, SE-100 44 Stockholm, Sweden (e-mail: mohamadreza.baradar@ee.kth.se; mrhesamzadeh@ee.kth.se; mehrdad.ghandhari@ee.kth.se).

Color versions of one or more of the figures in this paper are available online at http://ieeexplore.ieee.org.

Digital Object Identifier 10.1109/TPWRS.2013.2271871

$\boldsymbol{Q_{CONV}}$	Injected/absorbed reactive power vector of converters at PCCs.
$\boldsymbol{P_{DC}}$	Injected/absorbed active power vector at DC buses.
S_{Max,G_i}	Capacity limit of generator at bus i.
S_{Max,C_i}	Capacity limit of converter at bus i.
P_{lossc_i}	Converter block losses.
β	Scalar representing converter losses.

I. Introduction

INTRODUCTION of high voltage direct current (HVDC) technology has opened opportunities to transfer the electric power between two points which in particular are remotely located from each other.

Conventionally two types of converter, voltage source converters (VSCs) and current source converters (CSCs), are employed for two terminal HVDC links. The advances in power electronic devices and converter technology has led the multi terminal HVDC (MTDC) systems, which are not actually a new idea, to be suggested again as one of the solutions for interconnecting several generating and load points. In [1], the MTDC systems have been proposed as a cost-efficient way to connect offshore wind farms to the onshore AC systems. Due to practical reasons VSC is a more suitable option for building such hybrid AC-DC systems than its older generation, CSCs. The VSCs not only have no reactive power demand but also can either inject or absorb the reactive power to/from the AC grid in order to maintain AC side voltage as a generator [2]. The VSC technology can rapidly control active power and at the same time reactive power at each terminal independent of the DC power transmission [3]. Most importantly, the VSC does not need to reverse voltage polarity to change the direction of power flow in its DC link. As a results of advances in cable technology suitable for VSCs the power flow reversal is done by reversal of current direction. This characteristic allows several VSCs to be connected in parallel and form a meshed DC grid [4], [5]. Such hybrid AC-DC grids built from parallel connection of VSC links have a good potential to be used in the future bulk power systems [6]. Possibility of such connections has led to the proposition of European and North Sea SuperGrids that could connect several renewable energy sources to a common DC network [7], [8]. However, in order to fully reveal steady state and dynamic behavior of such systems to be used in the real-size power systems, extensive research has to be done. References [9] and [10] have investigated the fault occurrence in VSC MTDC grids and protection methodologies proposed to survive them. Studying the dynamic and transient behavior, modeling and control methodologies of VSC MTDC grids are the main focus of [11] and [12]. Two different power flow approaches, unified and sequential methods, for power flow calculation of VSC MTDC grids have been proposed by [13]–[15].

One of the key aspects of such a hybrid VSC AC-DC grid which has not been fairly addressed and reported in the literature is its impact on improving the economic efficiency of the electricity industry. It allows lower-cost generation to be substituted by the high-cost generation and it also improves the allocative efficiency by reducing the deadweight loss. In order to quantify these components of economic efficiency, these VSC AC-DC systems and their associated DC grids need to be modeled in the optimal power flow (OPF) formulation. Most of the OPF modelings proposed in the literature has accounted for CSC-HVDC links. In [16], [17], the sequential quadratic programming (SQP) and sequential gradient-restoration algorithm (SGRA) methods have been employed to solve AC-DC OPF of AC systems with multiterminal DC systems built from CSCs. Reference [18] has proposed a combined heuristic and interior point method (IPM) for solving the optimal reactive power flow (ORPF) problem in AC-DC systems incorporating CSC converters. In [19] a model for security-constrained unit commitment with CSC-type AC-DC systems using Benders decomposition has proposed in which the problem is divided into two subproblems which then solved using the mixed integer programming (MIP) and Newton Raphson (NR) methods.

However, since there are several major differences between VSCs and CSCs in both operation principle and structure, they cannot be applied to the AC-DC system incorporating VSCs. Most of the papers investigating OPF modeling of VSC converters has focused on VSC-based FACTS controllers embedded in AC systems [20]–[22]. In these studies, well known SQP and NR methods and predictor-corrector primal-dual interior point linear programming have been employed to solve the optimization problems. There are also little literature that has studied the OPF models incorporating two terminal VSC HVDC links. Reference [23] has modeled VSC HVDC links which are limited only to back-to-back VSC HVDC links in which the nonlinear set of AC-DC load flow equations are solved through the NR based OPF method. In [23], there is no DC grid representation and the DC links has been only accounted for by introducing an equation expressing that the total amount of active power injected into the DC system is equal to DC power losses. DC line losses have been also defined based on the DC slack bus voltage assuming that its value (i.e., $V_{DC,salck}$) is prespecified constant value before running the OPF. Also the control modes (i.e., PV or PQ mode) for each converter have been considered as constraint in OPF formulation. Recently, [24] has reported a security-constrained unit commitment (SCUC) which considers DC grids with VSC links. The Benders decomposition method has been used in [24]. Given the nonconvex nature of OPF problem, in all these studies, authors have tried to develop a convex optimization problem through several methods, these methods suffer from two main drawbacks: 1) loss of accuracy in results, and 2) complexity of algorithms. In our paper, a set of AC-DC constraints are developed through the line flow based (LFB) equations of power flow. In the LFB model the independent state variables includes bus voltage magnitudes, active and reactive line power flows [25]. These variables i.e. bus voltage magnitude and line power flows reflect more practical knowledge about the system than conventional power flow variables. Moreover, it is shown in this paper that this formulation make it possible to obtain a convex problem thanks to some small approximations we use in this paper. The LFB equations have been used for different studies in power system analysis. Reference [25] has formulated the power flow equations for load flow calculation

in radial AC systems with embedded FACTS devises. In [26] a LFB based formulation has been proposed for finding the optimal locations of TCSC using MIP. The authors in [26] suggest that some of the main equality constraints are replaced by inequality constraints in order for the problem to be solved through quadratic mixed-integer programming. Moreover, [26] have ignored the equation representing the transmission lines losses in order to remove the nonlinearity from the set of equations. The line power losses are the main origin of nonlinearity of power flow equations which some literature has presented losses as a quadratic function of difference phase angle of two connected buses and then used a linearized approximation of power losses [27], [28].

In our paper, we consider all nonlinear equations associated with active and reactive losses in all AC and DC lines as a functions of line flows variables. Instead of using a linearized approximation of power losses, we transform them to a conic constraint. Also, AC and DC line capacities and generator and VSC capacity limitations are all converted to the conic constraints.

After formulating the problem through the line flow variables, the problem is transformed to a second order cone programming (SOCP) format which is a convex problem and can be efficiently solved [29], [30]. Then through solving this convex problem, we obtain the global optimum point of the proposed formulation. It should be noted that there might be a small error between this solution and solution to the original problem due to the approximations used in this paper. Recently, several researchers have studied the possibility of redefinition and recasting of the nonlinear OPF problem as an SOCP programming or semidefinite programming problem under some mild conditions. Through their proposed formulation a globally optimal solution for the OPF problem can be obtained [31], [32].

In the proposed SOCP formulation of the AC-DC-OPF, unlike [23] in which the control modes are set before running the OPF and considered in the OPF formulation as constraint (exogenous modeling of control modes), the control modes [i.e., the point of common connection (PCC) as a PQ bus or PV bus and the a DC bus as DC slack bus] can be set either before OPF or after OPF solution is obtained (endogenous modeling of control modes). Therefore, based on the results obtained from our SOCP formulation of the AC-DC-OPF, one can determine which VSC set as PV or PQ mode and which DC bus is set as the slack bus.

In order to evaluate the accuracy of the proposed SOCP formulation of the AC-DC OPF, the numerical results which are obtained in GAMS platform using MOSEK solver [33] are compared to results obtained in MATPOWER software, [34]. The modified IEEE 30-bus test system is used as a case study.

II. VSC Station Model and Operation Modes

In a VSC-MTDC system with N converters, one converter should be considered as a DC slack converter to regulate its DC voltage around a specified value. For the sake of simplicity, the Nth VSC is considered as slack converter. This is to ensure the power balance in the MTDC network, i.e.,

$$P_{DC_1} + P_{DC_2} + \ldots + P_{DC_N} - P_{L,DC} = 0 \tag{1}$$

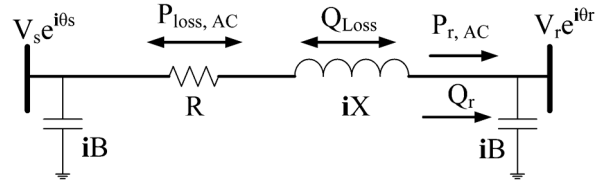

Fig. 1. Equivalent circuit of an AC line.

where P_{DC_i} is the injected DC power at each DC terminal and $P_{L,DC}$ is the total loss in the MTDC network. This implies that the active power at the PCC bus connected to a slack converter is not specified, and this unspecified power is defined by P_{CONV_N}. However, the converter N may control either the reactive power Q_{CONV_N} or the voltage V_{setN} at the PCC bus N. In [23], these control modes are set before running the OPF and considered in the OPF formulation as constraint.

However, in the AC-DC OPF proposed in this paper all active/reactive converter powers and voltage magnitudes at PCCs and DC buses are considered as independent control variables. Therefore, there is opportunity to either set these control variables as a prespecified constant values before running the AC-DC-OPF and solve the OPF with these constraints or obtain the specified values for these variables for which the objective function of AC-DC-OPF has been optimized. The slack converter also can be chosen based the output of AC-DC-OPF in such a way that the DC voltage value of a DC bus obtained from OPF solution can be set as the V_{setN} in load flow analysis.

III. AC-DC Line Flow Based Equations

In this section, the line flow equations [25] are extended to fully represent all AC and DC networks and converters.

A. AC Line Flow Equations

Fig. 1 shows the equivalent circuit of an AC line. Let consider a conventional direction for each line starting from sending bus and ending to receiving bus (see Fig. 1). The active and reactive power balance equations for AC node other than PCCs can be written as follows:

$$P_{G_i} - P_{D_i} = \sum_{j=1}^{n_{l_{AC}}} \boldsymbol{M_{PQ}}(i,j) P_{r,AC_j} + \sum_{j=1}^{n_{l_{AC}}} \boldsymbol{M_l}(i,j) P_{loss,AC_j} \tag{2}$$

$$Q_{G_i} - Q_{D_i} = \sum_{j=1}^{n_{l_{AC}}} \boldsymbol{M_{PQ}}(i,j) Q_{r_j} + \sum_{j=1}^{n_{l_{AC}}} \boldsymbol{M_l}(i,j) Q_{loss_j} - B_{i,i} V_i^2 \tag{3}$$

where

$$P_{loss,AC_j} = \frac{P_{r,AC_j}^2 + Q_{r_j}^2}{V_{r_j}^2} R_{j,j} \tag{4}$$

$$Q_{loss_j} = \frac{P_{r,AC_j}^2 + Q_{r_j}^2}{V_{r_j}^2} X_{j,j}. \tag{5}$$

Each element of $\boldsymbol{M_{PQ}}$ and $\boldsymbol{M_l}$ are as follows:

$$\boldsymbol{M_{PQ}}(i,j) = \begin{cases} -1 & \text{if bus i is the receiving end of line j} \\ 1 & \text{if bus i is the sending end of line j} \\ 0 & \text{if bus i is not connected to line j} \end{cases} \quad (6)$$

$$\boldsymbol{M_l}(i,j) = \begin{cases} 1 & \text{if bus i is the sending end of line j} \\ 0 & \text{otherwise.} \end{cases} \quad (7)$$

The equation associated with the voltage drop across each line is written as follows:

$$V_{s_j} e^{\mathbf{i}\theta_{s_j}} = V_{r_j} e^{\mathbf{i}\theta_{r_j}} + \frac{P_{r,AC_j} - \mathbf{i}Q_{r_j}}{V_{r_j} e^{-\mathbf{i}\theta_{r_j}}} (R_{j,j} + \mathbf{i}X_{j,j}). \quad (8)$$

If both sides of (8) are multiplied by $V_r e^{-\mathbf{i}\theta_r}$, then the magnitude of both sides are obtained and finally both sides are divided by V_r^2:

$$V_{s_j}^2 - V_{r_j}^2 = 2R_{j,j}P_{r,AC_j} + 2X_{j,j}Q_{r_j} + R_{j,j}P_{loss,AC_j} + X_{j,j}Q_{loss,AC_j} \quad (9)$$

therefore (9) can be written for each AC line.

To take into account the effect of phase angle in (8), we obtain the imaginary part of both sides in (8) and one can obtain the following equation by assuming $sin\theta_{sr} \approx \theta_{sr}$ and $V_s V_r \approx 1$:

$$\theta_{sr_j} = X_{j,j}P_{r,AC_j} - R_{j,j}Q_{r_j}. \quad (10)$$

On the other hand, a meshed power network can be seen as a graph consisting of n_c independent loops. According to graph theory, if $n_{l_{AC}}$ and $n_{b_{AC}}$ are assumed to be the number of branches and nodes of the graph, n_c can be obtained as follows:

$$n_c = n_{l_{AC}} - n_{b_{AC}} + 1. \quad (11)$$

The phase angle difference around each independent loop of a graph is zero. Therefore another set of equations associated with the graph loops (n_c equations) can be obtained using (10) as follows:

$$0 = \mathbf{CXP_{r,AC}} - \mathbf{CRQ_{r,AC}} \quad (12)$$

where $\mathbf{C}$ is an incidence matrix with the size of $n_c \times n_l$. This paper proposes set of (12) to model phase angle constraints for a meshed network. Although this approximation affects the accuracy of the OPF results, the algorithm becomes much simpler and faster. There are other works linearizing the voltage angle constraints around an operating point. This might result in a more accurate result however at higher computational time, [35]:

$$\boldsymbol{C}(i,j) = \begin{cases} 1 & \text{line j is in loop i with the same direction} \\ -1 & \text{line j is in loop i with the opposite direction} \\ 0 & \text{line j is not in loop i.} \end{cases} \quad (13)$$

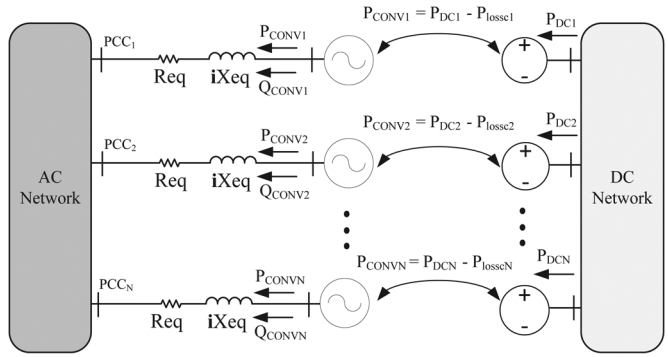

Fig. 2. Modeling of the AC-DC systems in the proposed OPF formulation.

B. Converters Equations

As in Fig. 2, converters can be modeled as a dummy generator or motor which either can absorb or inject active/reactive power to the AC network. The phase reactor and coupling transformer between PCCs and converters are also represented as an AC line with equivalent inductance and resistance. The active and reactive power balance equations at each PCC can be obtained as follows:

$$P_{G_i} - P_{D_i} + P_{CONV_i} = \sum_{j=1}^{n_{l_{AC}}} \boldsymbol{M_{PQ}}(i,j) P_{r,AC_j} + \sum_{j=1}^{n_{l_{AC}}} \boldsymbol{M_l}(i,j) P_{loss,AC_j} \quad (14)$$

$$Q_{G_i} - Q_{D_i} + Q_{CONV_i} = \sum_{j=1}^{n_{l_{AC}}} \boldsymbol{M_{PQ}}(i,j) Q_{r_j} + \sum_{j=1}^{n_{l_{AC}}} \boldsymbol{M_l}(i,j) Q_{loss_j} - B_{i,i} V_i^2 \quad (15)$$

where

$$P_{DC_i} = P_{CONV_i} + P_{lossc_i} \quad (16)$$

and if the converter losses are assumed to be proportional to passing active power through the converter (i.e. $P_{lossc_i} = \beta P_{CONV_i}$) the DC power at the DC bus at each station can be obtained as follows:

$$P_{DC_i} = (1+\beta) P_{CONV_i}. \quad (17)$$

C. DC Grid Equations

To derive the line flow equations for the DC grid, consider the equivalent circuit of DC line in Fig. 3. Each DC line are numbered from 1 to $n_{l,DC}$ and specified by an optional direction from sending bus to receiving bus (see Fig. 3). Doing so, active

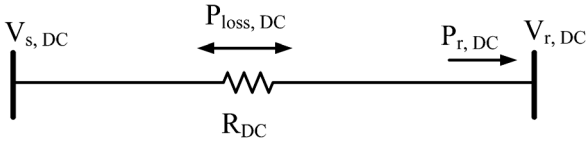

Fig. 3. Equivalent circuit of a DC line.

power balance equation at DC bus $n_{b,DC} = n_i$ is obtained based on the line flow variables shown in Fig. 3 as follows:

$$P_{DC_i} = -\sum_{j=1}^{n_{l_{DC}}} \boldsymbol{M_{P_{DC}}}(i,j) P_{r,DC_j} - \sum_{j=1}^{n_{l_{DC}}} \boldsymbol{M_{l_{DC}}}(i,j) P_{loss,DC_j} \quad (18)$$

where

$$P_{loss,DC_j} = \frac{P_{r,DC_j}^2}{V_{r,DC_j}^2} R_{DC_{j,j}}. \quad (19)$$

If we write the voltage drop equation for DC line $n_{l_{DC}} = n_j$, we have

$$V_{s,DC_j} = V_{r,DC_j} + \frac{P_{r,DC_j}}{V_{r,DC_j}} R_{DC_{j,j}}. \quad (20)$$

If both side of (20) are multiplied by V_{r,DC_j} and then get squared and finally are divided by V_{r,DC_j}^2 we reach

$$V_{s,DC_j}^2 = V_{r,DC_j}^2 + \frac{P_{r,DC_j}^2}{V_{r,DC_j}^2} R_{DC_{j,j}}^2 + 2P_{r,DC_j} R_{DC_{j,j}}. \quad (21)$$

From (19), equality (21) can be rewritten as

$$V_{s,DC_j}^2 - V_{r,DC_j}^2 = 2P_{r,DC_j} R_{DC_j} + P_{loss,DC_j} R_{DC_{j,j}}. \quad (22)$$

IV. Second-Order Cone Programming

An SOCP or conic optimization problem is a nonlinear convex problem which can be introduced as a general form of linear programming accompanied by nonlinear constraints which are in form of convex cones. Many kinds of problems such as LP and QP can be formulated as SOCPs and be efficiently solved through polynomial time IPMs [29], [30]. This optimization problem has the following form:

$$\begin{aligned} &\text{Min } \mathbf{F^T Xo} \\ &\text{subject to } \mathbf{AXo} = \mathbf{b} \\ &\qquad \underline{\mathbf{Xo}} \le \mathbf{Xo} \le \overline{\mathbf{Xo}} \\ &\qquad \mathbf{Xo} \in \kappa \end{aligned} \quad (23)$$

where $\mathbf{Xo} \in R^n$ is the optimization variable vector and $\mathbf{F}$ and $\mathbf{b}$ are constant vectors. If the variables are divided into $\mathbf{Xo} = [\mathbf{Xset}_1^T, \ldots, \mathbf{Xset}_p^T]^T$ in such a way that each element of $\mathbf{Xo}$ only belongs to one set of $\mathbf{Xset_i}$, then the additional condition, i.e., $\mathbf{Xo} \in \kappa$ is fulfilled if $\kappa = \{\kappa_i, \ldots, \kappa_p\}$ are convex cones and

$$\{\mathbf{Xo} \in R^n : \mathbf{Xset_i} \in \kappa_i, i = 1, \ldots, p\}. \quad (24)$$

Assuming $\mathbf{Xset_i} = [x_1, \ldots, x_{n_{set_i}}]^T$, each cone κ_i in (24) can have two following forms:

1) Second Order Cone: The standard form of this kind of cone is as follows:

$$\kappa_{SOC} = \left\{ \mathbf{Xo} \in R^{n_{set_i}} : x_1 \ge \sqrt{\sum_{j=2}^{n_{set_i}} x_j^2} \right\}. \quad (25)$$

2) Rotated Quadratic Cone: This kind of cone is obtained by rotating a κ_{SOC} with an angle of 45 degrees in $x_1 - x_2$ plane which has the following form:

$$\kappa_{RQC} = \left\{ \mathbf{Xo} \in R^{n_{set_i}} : 2x_1 x_2 \ge \sum_{j=3}^{n_{set_i}} x_j^2, x_1, x_2 \ge 0 \right\}. \quad (26)$$

Therefore if the constraints involves some linearly independent function and nonlinear inequality which can be transformed to form of κ_{SOC} and κ_{RQC}, the problem can be efficiently solved using IPMs.

V. Proposed SOCP Formulation for AC-DC-OPF

We assume the $\mathbf{F^T}$ in (23) to be the vector of short-run marginal cost for all exiting generating units in the system. We use this linear objective function, since the standard form of the conic problem shown in (23) has a linear objective function. However, one can use the piecewise linearization methods or other more accurate linear models for a cost objective functions. Let us define $\mathbf{Xo}$ vector as (27):

$$\boldsymbol{X}o = \left[\boldsymbol{W_{AC}^T}, \boldsymbol{W_{DC}^T}, \boldsymbol{P_{r,AC}^T}, \boldsymbol{Q_r^T}, \boldsymbol{P_{loss,AC}^T}, \boldsymbol{P_{loss,DC}^T}, \boldsymbol{P_G^T}, \boldsymbol{Q_G^T}, \boldsymbol{P_{CONV}^T}, \boldsymbol{Q_{CONV}^T}\right]^T \quad (27)$$

where $\boldsymbol{W_{AC}}$ is the vector of square of AC bus voltages $\boldsymbol{W_{DC}}$ is the vector of square of DC bus voltages. From derived (2), (3), (4), (5), (9), (12), (14), (15), (17), (18), (19) and (22) the constraint in the AC-DC OPF problem are as follows:

(A) Linear constraints:

$$\boldsymbol{P_G} - \boldsymbol{P_D} + \boldsymbol{P_{CONV}} - \boldsymbol{M_{PQ}} \boldsymbol{P_{r,AC}} - \boldsymbol{M_l} \boldsymbol{P_{loss,AC}} = 0 \quad (28)$$

$$\boldsymbol{Q_G} - \boldsymbol{Q_D} + \boldsymbol{Q_{CONV}} - \boldsymbol{M_{PQ}} \boldsymbol{Q_r} - \boldsymbol{M_l} \boldsymbol{Q_{loss}} - \boldsymbol{B} \boldsymbol{W_{AC}} = 0 \quad (29)$$

$$2\boldsymbol{R} P_{r,AC} + 2\boldsymbol{X} \boldsymbol{Q_r} + 2\boldsymbol{R} \boldsymbol{P_{loss,AC}} + 2\boldsymbol{X} \boldsymbol{Q_{loss}} - \boldsymbol{M_{W_{AC}}} \boldsymbol{W_{AC}} = 0 \quad (30)$$

$$\boldsymbol{\theta_{sr}} - \boldsymbol{X} \boldsymbol{P_{r,AC}} + \boldsymbol{R} \boldsymbol{Q_r} = 0 \quad (31)$$

$$\mathbf{C X P_{r,AC}} - \mathbf{C R Q_{r,AC}} = 0 \quad (32)$$

$$\boldsymbol{XP_{loss,AC}} - \boldsymbol{RQ_{loss}} = 0 \tag{33}$$

$$\boldsymbol{P_{DC}} - (1+\beta)\boldsymbol{P_{CONV}} = 0 \tag{34}$$

$$\boldsymbol{P_{DC}} + \boldsymbol{M_{PDC}P_{r,DC}} + \boldsymbol{M_{l_{DC}}P_{loss,DC}} = 0 \tag{35}$$

$$2\boldsymbol{R_{DC}P_{r,DC}} + \boldsymbol{R_{DC}P_{loss,DC}} - \boldsymbol{M_{W_{DC}}W_{DC}} = 0 \tag{36}$$

where (28) and (29) are associated with AC buses' mismatch constraints, (30) is associated with voltage drop equation constraint for AC lines, (31) is associated with phase angle difference on AC lines, (32) is associated with algebraic sum of phase angles in each independent loop, (33) represents the relation between active and reactive power losses at AC lines, (34) represents the relation between injected DC power at DC grid and converter power at PCC buses, (35) is associated with DC buses' mismatch constraints and finally (36) represents the DC voltage drop constraint on DC lines.

(B) Non-Linear constraints:

For each AC line $j = 1, \ldots, n_{l_{AC}}$:

$$P_{loss,AC_j} W_{r_{AC_j}} = \left(P^2_{r,AC_j} + Q^2_{r_j}\right) R_{j,j}. \tag{37}$$

For each DC line $j = 1, \ldots, n_{l_{DC}}$:

$$P_{loss,DC_j} W_{r_{DC_j}} = P^2_{r,DC_j} R_{DC_{j,j}} \tag{38}$$

where $W_{r_{DC_j}}$ and $W_{r_{AC_j}}$ are the square of DC and AC voltage at receiving end of line jth, $\boldsymbol{M_{W_{DC}}} = \boldsymbol{M^T_{P_{DC}}}$ and $\boldsymbol{M_{W_{AC}}} = \boldsymbol{M^T_{P_{AC}}}$. Since $W_{r_{DC_j}} \geq 0$, $P_{loss,DC_j} \geq 0$ and $W_{r_{AC_j}} \geq 0$, $P_{loss,AC_j} \geq 0$, if with a good approximation, the equality constraints (37) and (38) are replaced with inequality constraints, $(W_{r_{DC_j}}, P_{loss,DC_j}, P_{r,DC_j})$ and $(W_{r_{AC_j}}, P_{loss,AC_j}, P_{r,AC_j}, Q_{rj})$ form an appropriate set for each AC and DC line to be recast as a convex quadratic cone format and therefore introduced as a rotated quadratic cone in (26). For an arbitrary positive and sufficiently small constant $\epsilon \geq 0$, one can obtain

$$\begin{aligned} P_{loss,AC_j} W_{r_{AC_j}} &\geq \left(P^2_{r,AC_j} + Q^2_{r_j}\right) \frac{R_{j,j}}{(1+\epsilon)} \\ P_{loss,DC_j} W_{r_{DC_j}} &\geq P^2_{r,DC_j} \frac{R_{DC_{j,j}}}{(1+\epsilon)}. \end{aligned} \tag{39}$$

Inequalities in (39) can be rewritten as follows:

$$\begin{aligned} 2\tilde{P}_{loss,AC_j} W_{r_{AC_l}} &\geq P^2_{r,AC_j} + Q^2_{r_j} \\ 2\tilde{P}_{loss,DC_j} W_{r_{DC_l}} &\geq P^2_{r,DC_j} \end{aligned} \tag{40}$$

$$\begin{aligned} P_{loss,AC_j} &= \frac{2R_{j,j}}{(1+\epsilon)} \tilde{P}_{loss,AC_j} \\ P_{loss,DC_j} &= \frac{2R_{DC_{j,j}}}{(1+\epsilon)} \tilde{P}_{loss,DC_j}. \end{aligned} \tag{41}$$

Therefore (37) and (38) are replaced with (40) and (41). Doing so, the constraints involve linearly independent functions and nonlinear inequality with form of κ_{RQC} and then the problem can be efficiently solved using IPMs. It should be noted that the appropriate sets are replace by $(\tilde{P}_{loss,AC_j}, W_{r_{AC_j}}, P_{r,AC_j}, Q_{r_j})$ and $(\tilde{P}_{loss,DC_j}, W_{r_{DC_j}}, P_{r,DC_j})$. The other inequality constraints can be defined as follows:

$$\begin{aligned} &\text{for } i = 1, \ldots, n_{b_{AC}} \\ &\quad \underline{V}^2_{AC_i} \leq W_{AC_i} \leq \overline{V}^2_{AC_i} \\ &\quad \underline{P}_{G_i} \leq P_{G_i} \leq \overline{P}_{G_i} \\ &\quad \underline{Q}_{G_i} \leq Q_{G_i} \leq \overline{Q}_{G_i} \\ &\text{for } j = 1, \ldots, n_{l_{AC}} \\ &\quad \underline{P}_{r,AC_j} \leq P_{r,AC_j} \leq \overline{P}_{r,AC_j} \\ &\quad \underline{Q}_{r,AC_j} \leq Q_{r_j} \leq \overline{Q}_{r_j} \\ &\text{for } i = 1, \ldots, n_{b_{PCC}} \\ &\quad \underline{P}_{CONV_i} \leq P_{CONV_i} \leq \overline{P}_{CONV_i} \\ &\quad \underline{Q}_{CONV_i} \leq Q_{CONV_i} \leq \overline{Q}_{CONV_i} \\ &\text{for } i = 1, \ldots, n_{b_{DC}} \\ &\quad \underline{V}^2_{DC_i} \leq W_{DC_i} \leq \overline{V}^2_{DC_i} \\ &\text{for } j = 1, \ldots, n_{l_{DC}} \\ &\quad \underline{P}_{r,DC_j} \leq P_{r,DC_j} \leq \overline{P}_{r,DC_j}. \end{aligned} \tag{42}$$

The underline and overline signs are used for lower and higher limits, respectively. The present paper considers the ideal PQ-capability curve (PQ circle) for both generators and converters. For generator, we only consider PQ curve as a circle which is only based on armature current heating limit [36]. Taking into account all practical limitations will add more constraints to the optimization problem. Having used the ideal characteristic, their associated nonlinear inequality constraints can also be represented as a rotated quadratic cone as followa:

$$\begin{aligned} 2\hat{x}_{G_i}\tilde{x}_{G_i} &\geq P^2_{G_i} + Q^2_{G_i} \\ 2\hat{x}_{C_i}\tilde{x}_{C_i} &\geq P^2_{CONV_i} + Q^2_{CONV_i} \end{aligned} \tag{43}$$

where $\hat{x}_{G_i} = S^2_{Max,G_i}$, $\hat{x}_{C_i} = S^2_{Max,C_i}$, $\tilde{x}_{G_i} = \tilde{x}_{C_i} = 1/2$. The proposed SOCP formulation of the AC-DC-OPF is coded in GAMS platform and is solved through its MOSEK package [33]. This package is particularly very efficient in solving SOCP optimization problems via interior-point optimizer. The output numerical results obtained through MOSEK solver are compared to results obtained in MATPOWER software [34].

VI. Case Study and Simulation Results

Two cases are studied here; (A) The SOCP formulation of AC OPF problem, and (B) The SOCP formulation of AC-DC OPF problem.

A. SOCP Formulation of AC OPF

In this section, three example systems are studied. The OPF solutions of IEEE 14-bus, IEEE 30-bus, and IEEE 57-bus example systems are found using the SOCP formulation and

TABLE I
RESULTS FROM STANDARD FORMULATION (STRD) AND THE SOCP FORMULATION (SOCP) FOR THREE IEEE TEST SYSTEMS

IEEE Test System	14 Bus	30 Bus	57 Bus
Total Cost (STRD) ($)	5370.31	5926.87	25352.88
Total Cost (SOCP) ($)	5370.25	5924.42	25327.76
Error (%)	0.001	0.041	0.099

TABLE II
SOCP OPF AND STRD OPF RESULTS WHEN SOME LINES ARE CONGESTED (TEST CASE IEEE 30-BUS), * SHOWS THE CONGESTED CASES

Lines' Limit (MVA)	80*	60*	30*
Total cost (STRD) ($)	6063.91	6690.18	8692.26
Total cost (SOCP) ($)	6031.669	6606.892	8662.134
$P_{loss}(STRD)(MW)$	12.05	8.83	3.12
$P_{loss}(SOCP)(MW)$	12.239	9.198	3.159
$P_{loss}(LF)(MW)$	12.241	9.199	3.156
$Q_{loss}(STRD)(MVar)$	50.97	39.11	16.54
$Q_{loss}(SOCP)(MVar)$	51.611	40.612	16.671
$Q_{loss}(LF)(MVar)$	51.64	40.63	16.66

standard formulation of AC OPF. The SOCP formulation is coded in GAMS platform and solved using the MOSEK solver. The standard formulation of AC OPF is solved using the MATPOWER software [34]. The total generation costs, when there is no binding constraint, are given in Table I. This table shows 0.001% error for the IEEE 14-bus example system, 0.041% error for the IEEE 30-bus example system, and 0.099% error for the IEEE 57-bus example system.

The IEEE 30-bus example system is used to investigate the tightness of the SOCP relaxation and the loss over-satisfaction issue (Table II). First, the standard formulation and SOCP formulation of OPF problem are solved for 80-MVA, 60-MVA, and 30-MVA power flow limits. Then the results of SOCP formulation are fed into a load flow problem and the system loss is calculated. For the 80-MVA limit, two congested lines were observed. In this case, the ohmic loss from SOCP formulation is 12.239 MW and the ohmic loss from load flow calculation is 12.241 MW which is equivalent to 0.016% difference. In the second case, when we reduced the power flow limits to 60 MVA, three lines hit their limits. The SOCP formulation gives us better operating point as compared to the standard formulation while a difference of 0.01% in ohmic loss is observed. At the 30 MVA limit, five lines are congested. The ohmic losses calculated from the SOCP formulation and the load flow are 3.159 MW and 3.156 MW, respectively. This is equivalent to 0.095% difference in ohmic loss. Again in this case, the operation cost from SOCP formulation is less than the one from standard formulation. This issue of convex relaxation has been studied in a few literatures. Reference [37] studies some limitations of the semidefinite programming (SDP) relaxation of OPF problem especially those which are based on the conventional injection model [31]. Reference [38] shows that conic relaxation, i.e., replacing equality to inequality constraints is exact only for radial networks provided that there is no upper bound on active and reactive loads

TABLE III
RESULTS FROM STRD FORMULATION AND SOCP FORMULATION OF AC-DC OPF FOR IEEE 30-BUS TEST SYSTEM

	P_{G_i} (MW)		Q_{G_i} ($MVAR$)	
	STRD	SOCP	STRD	SOCP
G1	156.34	156.221	0	0
G2	140.00	140.00	8.11	7.868
G5	0	0	34.63	33.607
G8	0	0	38.67	39.444
G11	0	0	16.01	15.929
G13	0	0	24.00	24.00

	STRD	SOCP
Total Cost ($)	5926.87	5924.421
Total P-losses (MW)	12.94	12.821
Total Q-losses ($MVAR$)	54.17	53.601
Total P-Generation (MW)	296.34	296.221
Total Q-Generation ($MVAR$)	121.42	120.848
Total Q-Shunt ($MVAR$)	59.95	58.954

(load over-satisfaction). For a meshed network, authors in [39] show that if the phase angle constraints are eliminated from the original OPF problem and then the conic relaxation is applied, the obtained problem has an exact solution of the original problem provided some extra conditions are met. These conditions include no upper bound on active and reactive loads (load over-satisfaction) and successful angle recovery. They introduced some conditions under which the omitted phase angles can be recovered. It is shown that the phase angle recovery conditions are always valid for the tree networks, whereas it fails for the meshed networks in some cases. To handle this problem, they proposed installing a number of phase shifters in the meshed network to satisfy the phase angle recovery conditions. In our proposed SOCP formulation of OPF problem, we do not eliminate the phase angle constraints rather we incorporate them using a set of approximated equations given in (12). Also, we use loss over-satisfaction using the relaxation in (40) and (41) which is strongly related to the load over-satisfaction assumption. However as shown in Table II, even for low limits on power flows, the total power losses obtained in both standard OPF and SOCP OPF are very close. Negative nodal price is another issue discussed in the convex relaxation literature of OPF problem. Power markets operate at conditions with negative nodal prices with some regularity. Binding power flow constraints might create negative nodal prices. The relaxation in (40) and (41) appear to allow for increasing losses and thus prevent the occurrence of negative nodal prices. The detailed discussion of this issue has been left to the future extensions of this work.

B. SOCP Formulation of AC-DC OPF

To evaluate the proposed SOCP formulation of AC-DC-OPF, the IEEE 30-bus test system is modified and used. Since DC grid and their associated converters has not been implemented in MATPOWER software, only the results of proposed SOCP formulation for AC-OPF are used to be compared to results of AC OPF obtained in MATPOWER software. The detailed results obtained for IEEE 30-bus test system is given in Table III. As it

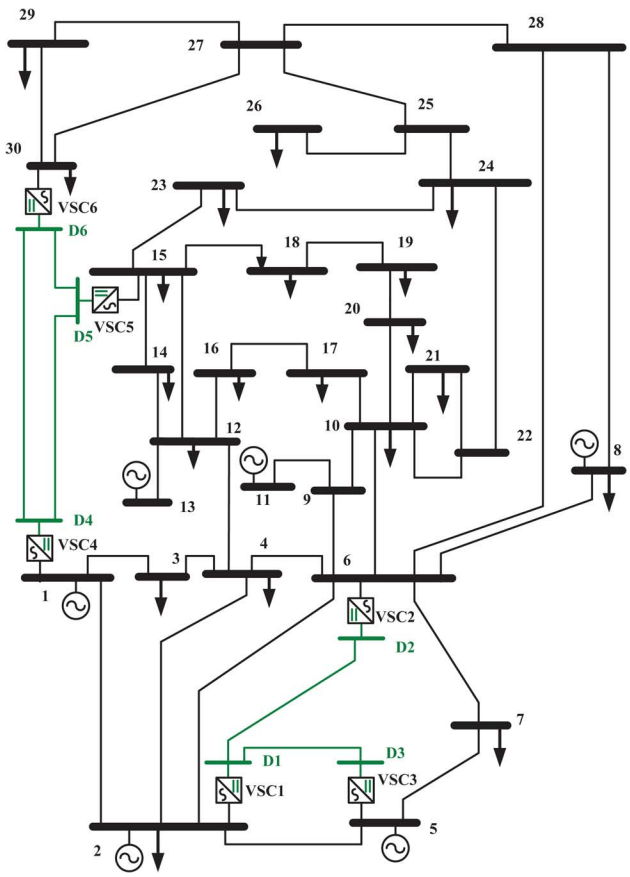

Fig. 4. Modified IEEE 30-bus test system with embedded DC system.

is seen the results are very close and this highlights the accuracy and correctness of the proposed SOCP formulation of AC-DC-OPF. It should be noted that active and reactive power and losses through each line which are variables in SOCP are almost identical. In order to implement the proposed SOCP formulation of AC-DC-OPF, the IEEE 30-bus test system with two installed three terminal DC system is used. This is shown in Fig. 4. This DC grid can have two different V and Delta configurations. Converters VSC1, VSC2, VSC3, VSC4, VSC5 and VSC6 are connected to AC buses 2, 6, 5, 1, 15 and 30, respectively. The DC voltage levels according to the ABB High Voltage Cable (HVC) product range are 80 kV, 150 kV and 320 kV [2]. In this paper, M9 module which has the highest voltage (320 kV) level is chosen for both cases. The converter power rating are chosen 100 (MVA). As it was mentioned, through the proposed OPF the PCCs can either set to be in one of the PV or PQ modes before running the OPF or active/reactive powers. AC voltage at PCC are considered as state variables and their final values from OPF are considered as economic values. Similarly, either an arbitrary DC bus can be set as the slack bus before running OPF or the DC slack is selected based on the OPF results. In our paper, none of the mentioned control modes are used for converters and only the boundary condition on converter variables are considered. Doing so, the converter variables are free to get a value for which the objective function is minimized. The OPF results are given in Tables IV and V. In Table IV, the $P-losses-DC$ is only the losses associated with DC lines. As

TABLE IV
RESULTS OF SOCP FORMULATION OF AC-DC-OPF FOR IEEE 30-BUS TEST SYSTEM WITHOUT (WO) AND WITH (W) TWO INSTALLED VSC-DC GRIDS

	P_{G_i} (MW)		Q_{G_i} $(MVAR)$	
	WO	W	WO	W
G1	156.221	150.44	0	0
G2	140.00	140.00	7.868	4.72
G5	0	0	33.607	6.24
G8	0	0	39.444	27.62
G11	0	0	15.929	9.53
G13	0	0	24.00	12.43

	WO	W
Total Cost ($)	5924.421	5798.57
Total P-losses (MW)	12.821	3.82
Total Q-losses $(MVAR)$	53.601	14.19
Total P-Generation (MW)	296.221	289.92
Total Q-Generation $(MVAR)$	120.848	36.16
Total Q-Shant $(MVAR)$	58.954	61.19
Total Q_{CONV} $(MVAR)$	0	43.00
Total P-losses-DC grid (MW)	0	2.10

TABLE V
RESULTS OF SOCP FORMULATION OF AC-DC-OPF FOR MTDC SYSTEM

DC Bus	**Voltage** $(p.u.)$	P_{CONV_i} (MW)	Q_{CONV_i} $(MVAR)$
D1	1.06	-79.96	17.31
D2	1.05	25.74	2.68
D3	1.04	52.53	26.89
D4	1.06	-59.91	-17.45
D5	1.05	40.44	10.07
D6	1.05	18.45	3.49

TABLE VI
RESULTS OF SOCP FORMULATION OF AC-DC-OPF FOR IEEE 30-BUS TEST SYSTEM WITH INSTALLED VSC DC GRIDS WITH CONVERTER RATING 50 MVA AND 100 MVA

Converter Rating (MVA)	50	100
Total Cost ($)	5808.94	5798.57
Total P-losses (MW)	5.39	3.82
Total Q-losses $(MVAR)$	20.86	14.19
Total P-Generation (MW)	290.45	289.92
Total Q-Generation $(MVAR)$	60.56	36.16
Total Q-Shant $(MVAR)$	60.60	61.19
Total Q_{CONV} $(MVAR)$	25.89	43.00
Total P-losses-DC grid (MW)	1.06	2.10

can be observed from the results due to economic allocation of converter variables the total AC losses are reduced which results in lower generated power and correspondingly lower generation cost. The reactive power generation also has been decreased due to local reactive power injected by converters.

In another analysis, the converter's rating powers are set to a lower value 50 (MVA) to see its impact on converter variables and total generation cost. The corresponding results are given in Tables VI and VII.

TABLE VII
RESULTS OF SOCP FORMULATION OF AC-DC-OPF FOR MTDC SYSTEM WITH INSTALLED VSC DC GRIDS WITH CONVERTER RATING OF 50 MVA AND 100 MVA

DC Bus	Voltage ($p.u.$)	P_{CONV_i} (MW)	Q_{CONV_i} ($MVAR$)	Converter Rating (MVA)
D1	1.06	-79.96	17.31	100
	1.06	-50.00	0	50
D2	1.05	25.74	2.68	100
	1.05	12.33	1.73	50
D3	1.04	52.53	26.89	100
	1.05	36.79	17.86	50
D4	1.06	-59.91	-17.45	100
	1.06	-49.56	-6.63	50
D5	1.05	40.44	10.07	100
	1.05	32.49	9.43	50
D6	1.05	18.45	3.49	100
	1.05	16.29	3.49	50

VII. CONCLUSION

This paper has successfully introduced SOCP in transforming nonlinear nonconvex AC-(VSC-)DC OPF problems into nonlinear convex problems. Comparing the introduced SOCP results with those from available commercial software (MATPOWER) proves the presented technique as an alternate reliable method for solving nonlinear non-convex AC-DC OPF equations. Through the proposed SOCP formulation of AC-DC OPF problem, several benefits of the DC systems with VSC technology can be evaluated.

REFERENCES

[1] W. Lu and B. Ooi, "Optimal acquisition and aggregation of offshore wind power by multi-terminal voltage-source HVDC," *IEEE Trans. Power Del.*, vol. 18, no. 1, pp. 201–206, Jan. 2003.

[2] P. Haugland, It's Time to Connect—Technical Description of HVDC Light Technology, ABB, Tech. Rep. 7, 2008.

[3] N. G. H. L. Gyugyi, *Understanding FACTS*. New York, NY, USA: Wiley-IEEE Press, 1999.

[4] N. Flourentzou, V. Agelidis, and G. Demetriades, "VSC-based HVDC power transmission systems: An overview," *IEEE Trans. Power Electron.*, vol. 24, no. 3, pp. 592–602, Mar. 2009.

[5] M. Bahrman and B. Johnson, "The ABCs of HVDC transmission technologies," *IEEE Power Energy Mag.*, vol. 5, no. 2, pp. 32–44, Mar.–Apr. 2007.

[6] T. J. Hamnmons *et al.*, "Role of hvdc transmission in future energy development," *IEEE Power Eng. Rev.*, pp. l0–25, Feb. 2000.

[7] D. V. Hertem and M. Ghandhari, "Multi-terminal VSC HVDC for the European supergrid: Obstacles," *Renew. Sustain. Energy Rev.*, vol. 14, no. 9, pp. 3156–3163, Dec. 2010.

[8] T. Vrana, R. Torres-Olguin, B. Liu, and T. Haileselassie, "The north sea super grid—A technical perspective," in *9th IET Int. Conf. AC and DC Power Transmission, 2010 (ACDC)*, Oct. 2010, pp. 1–5.

[9] J. Yang, J. Fletcher, and J. O'Reilly, "Multiterminal DC wind farm collection grid internal fault analysis and protection design," *IEEE Trans. Power Del.*, vol. 25, no. 4, pp. 2308–2318, Oct. 2010.

[10] L. Tang and B.-T. Ooi, "Locating and isolating DC faults in multi-terminal DC systems," *IEEE Trans. Power Del.*, vol. 22, no. 3, pp. 1877–1884, Jul. 2007.

[11] J. Liang, T. Jing, O. Gomis-Bellmunt, J. Ekanayake, and N. Jenkins, "Operation and control of multiterminal HVDC transmission for offshore wind farms," *IEEE Trans. Power Del.*, vol. 26, no. 4, pp. 2596–2604, Oct. 2011.

[12] S. Cole, J. Beerten, and R. Belmans, "Generalized dynamic VSC MTDC model for power system stability studies," *IEEE Trans. Power Syst.*, vol. 25, no. 3, pp. 1655–1662, Aug. 2010.

[13] M. Baradar, M. Ghandhari, and D. Van Hertem, "The modeling multi-terminal VSC-HVDC in power flow calculation using unified methodology," in *Proc. 2011 2nd IEEE PES Int. Conf. Exhib. Innovative Smart Grid Technologies (ISGT Europe)*, Dec. 2011, pp. 1–6.

[14] M. Baradar and M. Ghandhari, "A multi-option unified power flow approach for hybrid AC/DC grids incorporating multi-terminal VSC-HVDC," *IEEE Trans. Power Syst.*, to be published.

[15] J. Beerten, S. Cole, and R. Belmans, "Generalized steady-state VSC MTDC model for sequential AC/DC power flow algorithms," *IEEE Trans. Power Syst.*, vol. 27, no. 2, pp. 821–829, May 2012.

[16] C. Lu, S. Chen, and C. Ing, "The incorporation of HVDC equations in optimal power flow methods using sequential quadratic programming techniques," *IEEE Trans. Power Syst.*, vol. 3, no. 3, pp. 1005–1011, Aug. 1988.

[17] U. De Martinis, F. Gagliardi, A. Losi, V. Mangoni, and F. Rossi, "Optimal load flow for electrical power systems with multiterminal HVDC links," *Proc. Inst. Elect. Eng., Gen., Transm., Distrib. C*, vol. 137, no. 2, pp. 139–145, Mar. 1990.

[18] J. Yu, W. Yan, W. Li, C. Chung, and K. Wong, "An unfixed piecewise-optimal reactive power-flow model and its algorithm for AC-DC systems," *IEEE Trans. Power Syst.*, vol. 23, no. 1, pp. 170–176, Feb. 2008.

[19] A. Lotfjou, M. Shahidehpour, Y. Fu, and Z. Li, "Security-constrained unit commitment with AC/DC transmission systems," *IEEE Trans. Power Syst.*, vol. 25, no. 1, pp. 531–542, Feb. 2010.

[20] R. Palma-Behnke, L. Vargas, J. Perez, J. Nunez, and R. Torres, "Opf with SVC and UPFC modeling for longitudinal systems," *IEEE Trans. Power Syst.*, vol. 19, no. 4, pp. 1742–1753, Nov. 2004.

[21] X. Wei, J. Chow, B. Fardanesh, and A.-A. Edris, "A common modeling framework of voltage-sourced converters for load flow, sensitivity, and dispatch analysis," *IEEE Trans. Power Syst.*, vol. 19, no. 2, pp. 934–941, May 2004.

[22] Y. Xiao, Y. Song, and Y. Sun, "Power flow control approach to power systems with embedded FACTS devices," *IEEE Trans. Power Syst.*, vol. 17, no. 4, pp. 943–950, Nov. 2002.

[23] A. Pizano-Martinez, C. Fuerte-Esquivel, H. Ambriz-Perez, and E. Acha, "Modeling of VSC-based HVDC systems for a Newton-Raphson OPF algorithm," *IEEE Trans. Power Syst.*, vol. 22, no. 4, pp. 1794–1803, Nov. 2007.

[24] A. Lotfjou, M. Shahidehpour, and Y. Fu, "Hourly scheduling of DC transmission lines in SCUC with voltage source converters," *IEEE Trans. Power Del.*, vol. 26, no. 2, pp. 650–660, Apr. 2011.

[25] P. Yan and A. Sekar, "Analysis of radial distribution systems with embedded series FACTS devices using a fast line flow-based algorithm," *IEEE Trans. Power Syst.*, vol. 20, no. 4, pp. 1775–1782, Nov. 2005.

[26] G. Y. Yang, G. Hovland, R. Majumder, and Z. Y. Dong, "TCSC allocation based on line flow based equations via mixed-integer programming," *IEEE Trans. Power Syst.*, vol. 22, no. 4, pp. 2262–2269, Nov. 2007.

[27] H. Zhang, V. Vittal, G. Heydt, and J. Quintero, "A mixed-integer linear programming approach for multi-stage security-constrained transmission expansion planning," *IEEE Trans. Power Syst.*, vol. 27, no. 2, pp. 1125–1133, May 2012.

[28] N. Alguacil, A. Motto, and A. Conejo, "Transmission expansion planning: A mixed-integer LP approach," *IEEE Trans. Power Syst.*, vol. 18, no. 3, pp. 1070–1077, Aug. 2003.

[29] M. S. Lobo, L. Vandenberghe, S. Boyd, and H. Lebret, "Applications of second-order cone programming," *Linear Algebra Applicat.*, vol. 284, no. 1–3, pp. 193–228, 1998.

[30] F. Alizadeh and D. Goldfarb, "Second-order cone programming," *Math. Program. (Series B)* vol. 95, no. 1, pp. 3–51, 2003. [Online]. Available: http://rutcor.rutgers.edu/alizadeh/CLASSES/03sprNLP/Papers/allSurvey.pdf.

[31] J. Lavaei and S. Low, "Zero duality gap in optimal power flow problem," *IEEE Trans. Power Syst.*, vol. 27, no. 1, pp. 92–107, Feb. 2012.

[32] S. Bose, S. Low, and K. M. Chandy, "Equivalence of branch flow and bus injection models," in *Proc. 50th Annu. Allerton Conf. Communication, Control, and Computing*, Oct. 1–5, 2012.

[33] Gams/Mosek. [Online]. Available: http:www.gams.com/dd/docs/solvers/mosek.pdf.

[34] R. Zimmerman, C. Murillo-Sandnchez, and R. Thomas, "MATPOWER: Steady-state operations, planning, and analysis tools for power systems research and education," *IEEE Trans. Power Syst.*, vol. 26, no. 1, pp. 12–19, Feb. 2011.

[35] R. Jabr, "A conic quadratic format for the load flow equations of meshed networks," *IEEE Trans. Power Syst.*, vol. 22, no. 4, pp. 2285–2286, Nov. 2007.

[36] P. Kundur, *Power System Stability and Control*. New York, NY, USA: McGraw-Hill, 1994.

[37] B. Lesieutre, D. Molzahn, A. Borden, and C. DeMarco, "Examining the limits of the application of semidefinite programming to power flow problems," in *Proc. 2011 49th Annu. Allerton Conf. Communication, Control, and Computing (Allerton)*, 2011, pp. 1492–1499.

[38] M. Farivar, C. Clarke, S. Low, and K. Chandy, "Inverter var control for distribution systems with renewables," in *Proc. 2011 IEEE Int. Conf. Smart Grid Communications (SmartGridComm)*, 2011, pp. 457–462.
[39] M. Farivar and S. Low, "Branch flow model: Relaxations and convexification," in *Proc. 2012 IEEE 51st Annu. Conf. Decision and Control (CDC)*, 2012, pp. 3672–3679.

Mohamadreza Baradar (S'11) received the M.S. degree in electrical engineering from the University of Tehran, Tehran, Iran, in 2010. He is pursuing the Ph.D. degree at the Electric Power System Department of the Royal Institute of Technology (KTH), Stockholm, Sweden.

He is currently a member of the Electric Power System Department at KTH. His research interests include power system operation, electricity market, integration of renewable energy sources and AC/DC grids modeling.

Mohammad Reza Hesamzadeh (M'10) received the Ph.D. degree at Swinburne University of Technology, Australia.

He is an Assistant Professor in the Department of Electric Power Systems at KTH Royal Institute of Technology, Stockholm, Sweden. His special fields of interests include power systems planning and design, economics of wholesale electricity markets, and mathematical modelling and computing. He did his postdoctoral fellowship at KTH.

Dr. Hesamzadeh is a member of the International Association for Energy Economics (IAEE) and a member of the Cigre National Committee in Sweden.

Mehrdad Ghandhari (M'00) received the M.Sc. and Ph.D. degrees in electrical engineering from Royal Institute of Technology (KTH), Stockholm, Sweden, in 1995,and 2000, respectively. He is currently a full Professor at KTH. His research interests include power system dynamics, stability and control and FACTS and HVDC systems.